

Simulated impacts of insect defoliation on forest carbon dynamics

D Medvigy¹, K L Clark², N S Skowronski³ and K V R Schäfer⁴

¹ Department of Geosciences and Program in Atmospheric and Oceanic Sciences, Princeton University, 418B Guyot Hall, Princeton, NJ 08544, USA

² Silas Little Experimental Forest, USDA Forest Service, 501 Four Mile Road, New Lisbon, NJ 08064, USA

³ USDA Forest Service, Northern Research Station, 180 Canfield Street, Morgantown, WV 26505, USA

⁴ Department of Biological Sciences, Rutgers University, 195 University Avenue, Newark, NJ 07102, USA

E-mail: dmedvigy@princeton.edu

Received 31 July 2012

Accepted for publication 18 October 2012

Published 6 November 2012

Online at stacks.iop.org/ERL/7/045703

Abstract

Many temperate and boreal forests are subject to insect epidemics. In the eastern US, over 41 million meters squared of tree basal area are thought to be at risk of gypsy moth defoliation. However, the decadal-to-century scale implications of defoliation events for ecosystem carbon dynamics are not well understood. In this study, the effects of defoliation intensity, periodicity and spatial pattern on the carbon cycle are investigated in a set of idealized model simulations. A mechanistic terrestrial biosphere model, ecosystem demography model 2, is driven with observations from a xeric oak–pine forest located in the New Jersey Pine Barrens. Simulations indicate that net ecosystem productivity (equal to photosynthesis minus respiration) decreases linearly with increasing defoliation intensity. However, because of interactions between defoliation and drought effects, aboveground biomass exhibits a nonlinear decrease with increasing defoliation intensity. The ecosystem responds strongly with both reduced productivity and biomass loss when defoliation periodicity varies from 5 to 15 yr, but exhibits a relatively weak response when defoliation periodicity varies from 15 to 60 yr. Simulations of spatially heterogeneous defoliation resulted in markedly smaller carbon stocks than simulations with spatially homogeneous defoliation. These results show that gypsy moth defoliation has a large effect on oak–pine forest biomass dynamics, functioning and its capacity to act as a carbon sink.

Keywords: defoliation, carbon budget, New Jersey Pine Barrens, ecosystem demography model, gypsy moth

1. Introduction

Recent studies using atmospheric CO₂ observations and inverse modeling have inferred a terrestrial carbon sink of several petagrams of carbon (Pg C) per year over the past

few decades (Le Quéré *et al* 2009, Beaulieu *et al* 2012), and forest inventory-based analyses have identified a net sink in boreal and temperate forests of 1.2 Pg C yr⁻¹ since 1990 (Pan *et al* 2011). However, there is substantial regional and temporal variability in this C sink. In temperate ecosystems, this variability is at least in part due to disturbance, including insect epidemics (Kurz *et al* 2008a, 2008b, Amiro *et al* 2010, Pfeifer *et al* 2011, Hicke *et al* 2012). As one example, gypsy moth (*Lymantria dispar* L.) outbreaks are a risk throughout the northern hemisphere, including Canada, Europe and Japan



Content from this work may be used under the terms of the [Creative Commons Attribution-NonCommercial-ShareAlike 3.0 licence](http://creativecommons.org/licenses/by-nc-sa/3.0/). Any further distribution of this work must maintain attribution to the author(s) and the title of the work, journal citation and DOI.

Table 1. Evaluation of ED2 at Silas Little Experimental Forest.

Dataset	Units	Observed	Simulated
Net ecosystem productivity ^a	tC ha ⁻¹	10.0	11.2
Nighttime-only net ecosystem productivity ^a	tC ha ⁻¹	-10.2	-9.2
Hardwood basal area increment ^b	m ² ha ⁻¹	1.06	1.12
Conifer basal area increment ^b	m ² ha ⁻¹	0.06	0.06
Hardwood basal area mortality ^b	m ² ha ⁻¹	5.6	5.1
Conifer basal area mortality ^b	m ² ha ⁻¹	0.02	0.02

^a Cumulative, 2005–9.

^b Difference between autumn 2009 and autumn 2005.

(Johnson *et al* 2005). Over 41 million m² of basal area in the northeastern US are thought to be at risk of attack by gypsy moth, and thus far gypsy moths have invaded about 23% of the forested area that provides suitable habitat for them throughout the US (Hicke *et al* 2012).

Field observations and remote sensing are increasing our ability to detect these attacks, and to assess the implications for ecosystem structure and functioning (Liebhold *et al* 1992, Barron and Patterson 2008, de Beurs and Townsend 2008, Schäfer *et al* 2010). Such observations are critical for the development and testing of predictive, mechanistic numerical models of the terrestrial biosphere. At one measurement site where a gypsy moth defoliation event was well-observed, numerical experiments that did not include gypsy moth defoliation failed to realistically simulate the observations of CO₂ fluxes and tree growth and mortality rates (Miao *et al* 2011, Scheller *et al* 2011).

Here, we seek to build on our understanding of forest responses to gypsy moth defoliation. Because there has been relatively little research on the impacts of gypsy moth defoliation on the carbon cycle, we work in an idealized setting, and focus on understanding the chains of events, processes and mechanisms, rather than attempting to predict the specific future trajectory of a forest. Consequently, we ignore potentially confounding factors including climate change, fires and land-use change. The test-bed for our analysis is the Silas Little Experimental Forest (39.9°N, 74.6°W), chosen because gypsy moth defoliation was observed in detail at this site (Schäfer *et al* 2010, Clark *et al* 2010). We describe how a terrestrial biosphere model was modified to enable it to represent defoliation events and then evaluate the model against eddy-flux and biometry measurements. We use the model to address the following questions. (1) What is the response of the carbon cycle to defoliation events of varying intensity? (2) How does the carbon cycle respond to the periodicity of defoliation events? (3) Is the spatial representation of defoliation important?

2. Methods

Our analysis was underpinned by recent observations at the Silas Little Experimental Forest (SLEF), located in Pemberton Township in the Pine Barrens of southern New Jersey, USA (39.9°N, 74.6°W). Detailed descriptions of the site already exist (Skowronski *et al* 2007, Clark *et al* 2010, Schäfer *et al*

2010). The site's mean annual temperature is 11.5 °C, and its mean annual precipitation is 1123 mm. The soil is derived from Cohansey sands, and has low nutrient content and cation exchange capacity (Schäfer 2011). The study area is relatively flat with a mean elevation of 33 m. The dominant tree species are *Quercus prinus* Willd. (chestnut oak), *Quercus velutina* Lam. (black oak) and *Quercus coccinea* Munchh. (scarlet oak), with scattered *Pinus rigida* Mill. (pitch pine) and *Pinus echinata* Mill. (shortleaf pine).

In 2007, the site was completely defoliated by gypsy moth from the end of May until mid-July (Clark *et al* 2010, 2012, Schäfer *et al* 2010, Schäfer 2011). Following the cessation of herbivory, leaf area recovered to about 50% of the summer maxima that had occurred in 2005 and 2006. This defoliation event was probably unusually intense because the pines (then comprising about 27% of the live basal area) were defoliated and the plastic flagging on some of the trees was eaten. In the few years following defoliation, approximately 1/3 of the oaks (on a basal area basis) experienced mortality (table 1), although the different oak species varied in their ability to recover from the attack (Schäfer 2011). The pines exhibited little mortality following defoliation (table 1), and their recovery may have been facilitated by epicormic budding. Other areas of the New Jersey Pine Barrens were defoliated in 2007. At pine–oak and pine–scrub oak stands, oaks but not pines were defoliated (Clark *et al* 2010). Other studies have also indicated that oak is preferred over pine by the gypsy moth (Campbell and Sloan 1977, Davidson *et al* 2001, Barron and Patterson 2008).

Our modeling was carried out with the ecosystem demography 2 model (ED2) (Medvigy *et al* 2009, 2010). The model uses a system of size- and age-structured partial differential equations to closely approximate the first moment behavior of a corresponding individual-based stochastic gap model to realistically represent fine-scale heterogeneity in ecosystem structure within each grid cell. ED2 differs from most other large-scale terrestrial models by formally scaling up physiological processes through vegetation dynamics to ecosystem scales, while simultaneously modeling fires, natural disturbances, land use and the dynamics of recovering lands (Moorcroft *et al* 2001, Hurtt *et al* 2002, Albani *et al* 2006).

Several important modifications were made to ED2 for this study. First, although ED2 has previously been shown to accurately simulate eddy-flux measurements and tree growth and mortality measurements throughout the northeastern US

Table 2. Parameters defining the xeric plant functional types (PFTs) used in this study. ‘M09 name’ gives the name used for the parameter in Medvigy *et al* (2009).

Parameter name	Units	M09 name	Applicable PFT	Value
Photosynthetic capacity per unit leaf area	$\mu\text{mol m}^{-2} \text{s}^{-1}$	V_{m0}	Xeric hardwoods	25.1
Photosynthetic capacity per unit leaf area	$\mu\text{mol m}^{-2} \text{s}^{-1}$	V_{m0}	Xeric conifers	10.5
Growth respiration fraction	—	r_g	Xeric hardwoods	0.12
Fine root turnover rate	yr^{-1}	α_{root}	Xeric hardwoods and xeric conifers	2.8
Water availability parameter	$\text{m}^2 \text{yr}^{-1} (\text{kg root})^{-1}$	K_W	Xeric hardwoods and xeric conifers	2500

(Medvigy *et al* 2009, Medvigy and Moorcroft 2012), the model was never specifically evaluated for xeric sites such as SLEF, and did not include plant functional types (PFTs) for xeric habitats. Unsurprisingly, preliminary analysis indicated that ED2 did not capture net ecosystem productivity at SLEF as accurately as for mesic sites. We addressed this by introducing two new PFTs, a xeric hardwood and a xeric conifer. Whittaker and Woodwell (1968) derived allometric relationships for the species characteristic of the xeric northern coastal plain, and we use their *Quercus coccinea* allometry for our xeric hardwood and their *Pinus rigida* allometry for our xeric conifer. With the additional exceptions of the parameters noted in table 2, the parameterizations for the xeric hardwood and xeric conifer were set to be identical to ED2’s existing parameterizations for mesic mid-successional hardwoods and mesic northern pines, respectively.

A second new aspect developed in this work was the characterization of a defoliation event in ED2, done through ED2’s already-existing capability of representing sub-grid-scale heterogeneity related to disturbance (Albani *et al* 2006, Medvigy *et al* 2009). For example, suppose that the landscape initially consists of N sub-grid-scale tiles. To simulate a defoliation event, each of the N tiles is split into two daughter tiles. One of the tiles is set to be of size f relative to its parent tile, and the other daughter tile is set to be of relative size $1 - f$. The tile of relative size f will undergo complete defoliation of all trees (see below), regardless of tree size, age, or previous disturbance history. The tile of relative $1 - f$ remains completely undisturbed throughout the defoliation event. We subsequently refer to f as the ‘defoliation intensity’. This procedure has the effect of doubling the number of tiles at each defoliation event, and this can lead to a computationally unwieldy number of tiles. The model therefore periodically reviews all tiles and merges tiles with similar forest composition and structure.

The temporal evolution of defoliation events was derived by using observations from SLEF. Although only measurements of maximum seasonal leaf area index (LAI) are available, sap flow and LiDAR observation, ongoing since 2005, can be used to infer the seasonal trajectory of LAI (Clark *et al* 2012). One possibility would be to prescribe the inferred 2007 LAI time series (figure 1) for any simulated year in which SLEF experiences a gypsy moth outbreak. However, in long-term simulations spanning years and decades, there will be changes in the simulated structure and composition of SLEF, as well as the maximum potential LAI. To deal with the possibility of changes in maximum potential LAI, we defined the relative LAI as the ratio of the 2007 LAI to

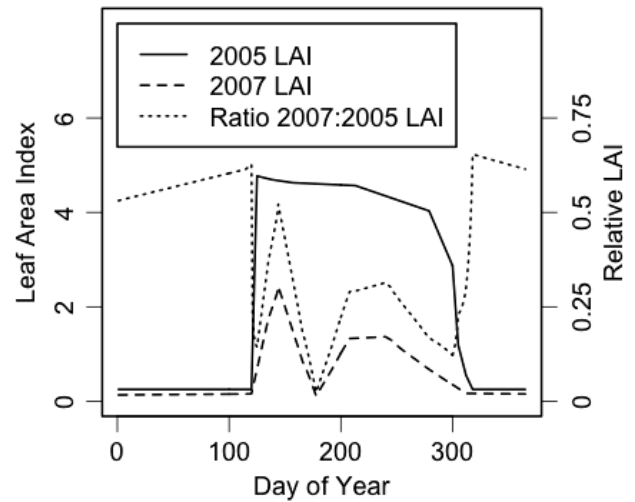


Figure 1. Seasonal leaf area index (LAI) at Silas Little Experimental Forest. A defoliation event occurred in 2007.

the 2005 LAI (figure 1). In years with simulated gypsy moth outbreaks, the realized LAI was taken to be the product of the maximum potential LAI and the 2007:2005 relative LAI. In years without defoliation, the timing of leaf expression follows the 2005 observations (figure 1), and trees are able to attain their maximum potential LAI.

Of central interest here is the model’s parameterization of mortality. The central unit of ED2 is the ‘cohort’: the density of trees of a given plant functional type, size (with separate leaf, fine root, sapwood and heartwood biomass pools), and disturbance history. The ‘forest’ in the model typically consists of a collection of cohorts that dynamically evolves over time. Mortality, applied on a monthly time step, acts by decrementing cohort number density. The mortality rate depends on a cohort’s carbon balance. When a cohort is in positive overall carbon balance, mortality proceeds at a small, background rate. However, mortality rates can become large if the cohort is in negative or nearly negative carbon balance. In the model, the gypsy moth does not directly kill trees. Instead, defoliation is modeled by reducing the size of an affected cohort’s leaf biomass pool. If the cohort consequently falls into an unfavorable carbon balance, it will then experience large mortality rates. For further details on mortality in ED2, see Albani *et al* (2006).

In a preliminary analysis, we found that this parameterization enabled the model to give satisfactory simulations of net ecosystem productivity, tree diameter growth and tree mortality for the 2005–9 period at SLEF, which included the

Table 3. Summary of the defoliation simulations analyzed in this study.

Simulation name	Defoliation intensity (%)	Defoliation periodicity (yr)	Spatial representation of defoliation
I0	None	None	None
I10-P5	10	5	Heterogeneous
I20-P5	20	5	Heterogeneous
I30-P5	30	5	Heterogeneous
I40-P5	40	5	Heterogeneous
I50-P5	50	5	Heterogeneous
I60-P5	60	5	Heterogeneous
I40-P10	40	10	Heterogeneous
I40-P15	40	15	Heterogeneous
I40-P25	40	25	Heterogeneous
I40-P40	40	40	Heterogeneous
I40-P60	40	60	Heterogeneous
I40-P5-HOM	40	5	Homogeneous

gypsy moth outbreak in 2007 (table 1). In particular, the model simulated the observed basal area mortality to within 10%. In the model, almost all of this mortality was attributable to the 2007 gypsy moth outbreak.

All simulations were carried out for a single model grid cell. The grid cell is intended to represent the approximate footprint of the SLEF eddy-flux tower (1 km²), but the size of the grid cell does not affect model results. The meteorological forcing, initial stand structure and composition, and soil texture are assumed to be the same for the entire grid cell. The simulations were initialized with the observed ecosystem structure and composition at SLEF from 2005 and were integrated forward for 200 yr. Soil carbon, litter and woody debris were initialized from observed values (Clark *et al* 2010, Schäfer 2011). Because only 6 yr of site-level meteorological observations were available at the time of this writing (corresponding to the years 2005–10), we simply recycled this 6 yr forcing dataset over the course of the 200 yr simulations. The 6 yr forcing dataset contained a very wet growing season (2009; 499 mm from 15 May to 15 Oct) and a very dry growing season (2010; 350 mm from 15 May to 15 Oct), thus representing a wide range of conditions occurring in the New Jersey Pine Barrens.

We carried out 3 sets of simulations to investigate the effects of defoliation intensity, defoliation periodicity and spatial pattern of defoliation. (i) Intensity experiments: the fraction of the grid cell that was defoliated varied among simulations, and ranged from 0% to 60% (see table 3). For simplicity, we assume that defoliated trees become completely defoliated. Also, because hardwood trees have been most severely affected by historical gypsy moth outbreaks (Davidson *et al* 2001, Barron and Patterson 2008), we assume that only the hardwoods are defoliated. In each of these experiments, defoliation was prescribed to occur every 5 yr. This is consistent with observational records, which indicate a 5 yr periodicity in 1 km × 1 km quadrats in xeric oak–pine forests of the northeastern US (Johnson *et al* 2006). (ii) Periodicity experiments: defoliation was prescribed at 40% intensity in each simulation, comparable to historical defoliation events (Johnson *et al* 2006), but the periodicity of defoliation varied from 5 to 60 yr. We again assume that all

defoliated trees are completely defoliated, and that only the hardwoods are defoliated. (iii) Spatial pattern: we investigated if a partial defoliation of all trees in the grid cell would differ from complete defoliation of some trees and leaving others completely intact. Depending on the size of the grid cell, both situations can be realistic. At the level of the forest stand, outbreaks are spatially heterogeneous and often out-of-sync (Johnson *et al* 2006), while on large spatial scales outbreaks are more synchronous (Peltonen *et al* 2002). This comparison is also of interest because many terrestrial biosphere models run at coarse resolutions (e.g., 100–200 km) and do not represent spatial heterogeneity very well. A potential way for these models to represent defoliation would be a partial defoliation of all trees in the coarse grid cell. This aggregation is also apparent when attempting to use spectral reflectance and derived data products (NDVI, GPP, etc) from satellite observations with low spatial resolution, such as MODIS. We therefore created an alternate defoliation prescription consisting of a weighted average of the 2005 (60%) and 2007 (40%) LAI profiles, and applied this to all trees in the grid cell with a 5 yr defoliation periodicity.

Simulations are named according to their intensity and periodicity; e.g., 40% defoliation with 5 yr periodicity would be named I40-P5. All simulations use the default heterogeneous representation of defoliation unless explicitly suffixed by ‘-HOM’ to denote homogenous representation of foliage. This notation is summarized in table 3.

3. Results and discussion

3.1. Intensity of defoliation

In all simulations, long-term net ecosystem productivity (NEP; equal to photosynthesis minus respiration) takes on positive values for well over a century, indicating that SLEF continues to act as a carbon sink regardless of defoliation (figure 2(a)). The transient behavior is similar in the different simulations and is characterized by rapidly increasing NEP over the first 10–20 yr, stabilizing, and finally a slow decline beginning by about year 60. There is a clear ordination of the NEP time series corresponding to defoliation intensity,

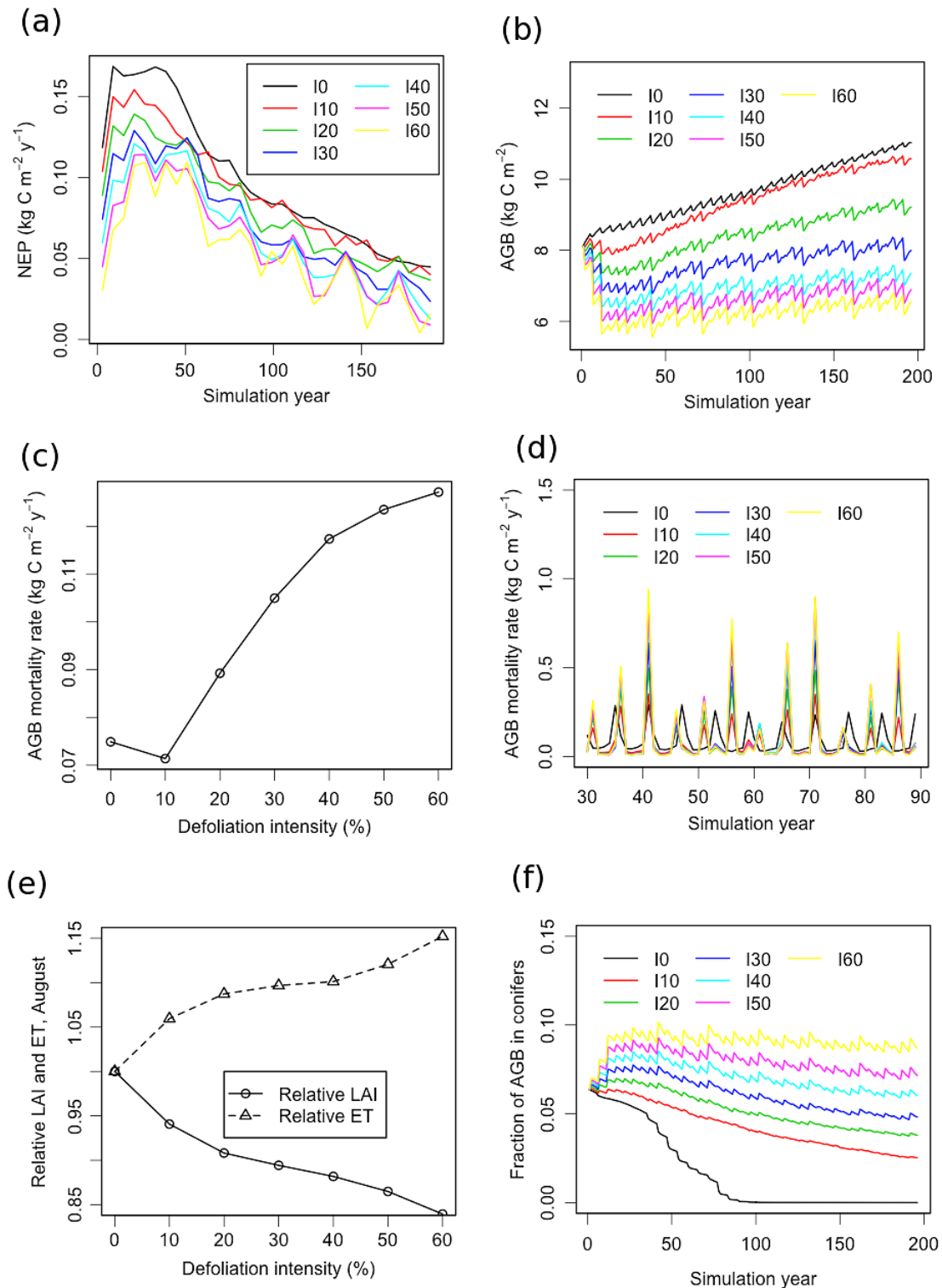


Figure 2. Impacts of defoliation intensity on ecosystem structure and functioning. In all simulations, defoliation periodicity is 5 yr. (a) Time series of net ecosystem productivity (NEP). To improve legibility, NEP is presented as 6 yr averages. (b) Time series of live aboveground biomass (AGB). (c) Simulation-averaged AGB mortality rates. (d) Aboveground biomass (AGB) mortality rate for simulation years 31–90. These years were extracted only to improve legibility; the entire time series has a 6 yr cycle of mortality for simulation I0 and a 5 yr cycle of mortality for other simulations. (e) August leaf area index (LAI) and evapotranspiration per unit leaf area (ET). LAI and ET are averaged over the simulations and shown relative to I0. (f) Time series of the fraction of conifer AGB to the total AGB of all tree species.

with I0 generally having the largest NEP and I60-P5 the smallest NEP (figure 2(a)). Simulation-averaged NEP decreases approximately linearly with disturbance intensity at

a rate of about $7 \text{ g C m}^{-2} \text{yr}^{-1}$ for every 10% of defoliation. Note that the figure shows NEP averaged in 6 yr bins to enhance the legibility of the long-term trends. NEP does take

on negative values in some years, especially those years with large defoliation intensity.

Our results can be compared to Edburg *et al* (2011), who simulated forest recovery from a mountain pine beetle outbreak. Whereas the simulations presented here prescribe periodic defoliation, their simulations prescribed a single mortality event near the simulation start time. They found that 50% mortality would result in an NEP anomaly of about $-50 \text{ g C m}^{-2} \text{ y}^{-1}$ in the decade following the outbreak. This anomaly is quite similar to the approximately $-70 \text{ g C m}^{-2} \text{ y}^{-1}$ anomaly between our I50-P5 and I0 despite the aforementioned differences in simulation design.

We find a nonlinear relationship between aboveground live biomass (AGB) and defoliation intensity (figure 2(b)). The 200 yr time series from I0 and I10-P5 are generally closely matched, but then there is a wide gap between I10-P5 and I20-P5, and finally the simulations with the largest defoliation intensities (I40-P5, I50-P5, I60-P5) are generally clustered together. In the model, changes in AGB are determined as the balances between gains (tree growth and recruitment) and losses (mortality). We examined the time series of growth, recruitment, and mortality, and found that the mortality term (figure 2(c)) had the largest nonlinear response to defoliation intensity. Simulation-averaged mortality was nearly equal in I0 and I10-P5, increased as intensity increased from 10% to 40%, and then increased at a slower rate as intensity increased from 40% to 60%. This is consistent with the differences in live AGB among simulations (figure 2(b)). Interestingly, Baker (1941) also showed a nonlinear increase in mortality with defoliation intensity, however in the cases studied there, the response was not as gradual as the modeled response in this investigation (figure 2(c)).

We also identified interactions between defoliation intensity and drought. Mortality rates during years 30–89 are shown in figure 2(d). In all simulations with defoliation, there is a spike in mortality every 5th year, in accord with the disturbance frequency. However, I0 has spikes in mortality in every 6th year, corresponding to years with meteorological forcing based on 2010 observations. That summer was New Jersey's hottest and 8th driest since records began in 1895.⁵ Because I0 had the smallest late summer evapotranspiration per unit leaf area (figure 2(e)), it had warmer leaves than the other simulations. The higher foliar temperatures led to increased water stress, and the water stress ultimately led to increased mortality. This is consistent with a previous study that investigated the interactive effect of drought and defoliation (Bréda and Badeau 2008).

Insect defoliation has a strong effect on simulated ecosystem composition. We expected that the xeric conifers would eventually die out in all simulations because they require fire for germination, and our simulations did not include fire. Without insect disturbance, conifers indeed become locally extinct by around year 85 of the simulation (figure 2(f)). However, because the defoliation selectively impacts the oaks, it gives a competitive advantage to

conifers, and the persistence of conifers is much stronger in the simulations with defoliation. Conifer biomass actually increases as a proportion of the total for the first few decades in simulations with defoliation intensities of 30% or larger (figure 2(f)). Some historical records have shown similar behavior with differential species responses to climatic and biotic events, thus changing species composition over time (Albertson and Weaver 1945). Nevertheless, the simulations probably overstate the actual ability of pines to capitalize on oak defoliation because pines are more susceptible to windthrow and lightning when the canopies of the larger oaks are reduced, and this is not accounted for in the simulations. Furthermore, defoliation of pines has been observed to occur during unusually extreme outbreaks in the New Jersey Pine Barrens, and this was not accounted for by the model.

3.2. Periodicity of defoliation

There was a strong nonlinear response of the carbon cycle to defoliation periodicity. When averaged over the 200 yr simulation, both gross primary productivity (GPP) and total ecosystem respiration (R_{tot}) responded positively to increasing periodicity, but the stronger response of GPP drove increases in NEP (figure 3(a)). NEP increases by over 40% as defoliation periodicity increases from 5 to 15 yr, but additional increases in periodicity have a comparatively small effect on NEP. This model prediction suggests that there is a compounding effect of defoliation that is mainly operative for periodicities shorter than 15 yr, and is similar to previous findings that individual oak trees in New England require about 10 yr to recover from a single heavy defoliation event (Campbell and Sloan 1977). However, at nutrient-poor sites, the timescale to recovery may be longer if there is a lag before canopy nitrogen content returns to pre-defoliation levels. Such nutrient dynamics were not implemented in our simulations.

The end-of-simulation live AGB values also increased by over 40% as defoliation periodicity increased from 5 to 15 yr, and end-of-simulation live AGB was insensitive to additional increases in periodicity (figure 3(b)). However, increasing defoliation periodicity from 15 to 60 yr was associated with increases in the live AGB in the largest trees, and decreases in the live AGB of intermediate size classes. Furthermore, increasing defoliation periodicity was also correlated with decreases in conifer fraction; the I40-P5 end-of-simulation conifer fraction was 6% (compare figure 2(f)), while in I40-P60, conifers became locally extinct by about year 115.

3.3. Spatial structure of disturbance

Comparing homogenous (i.e. suffix HOM in the simulation, figure 4) versus heterogeneous defoliation events whereby a different fraction of foliage is consumed showed a large spatial and temporal variability. The 'I40-P5-HOM minus I40-P5' difference in annual NEP is presented in figure 4(a), and is a substantial fraction of total NEP in I40-P5 (see figure 2(a)). A spectral analysis found that most of the power was in the 5 yr and 6 yr cycles, which are associated with the defoliation and meteorological forcing, respectively.

⁵ NJ State Climatologist, <http://climate.rutgers.edu/stateclim/?section=menu&%20target=aug10>, downloaded on 8 May 2012.

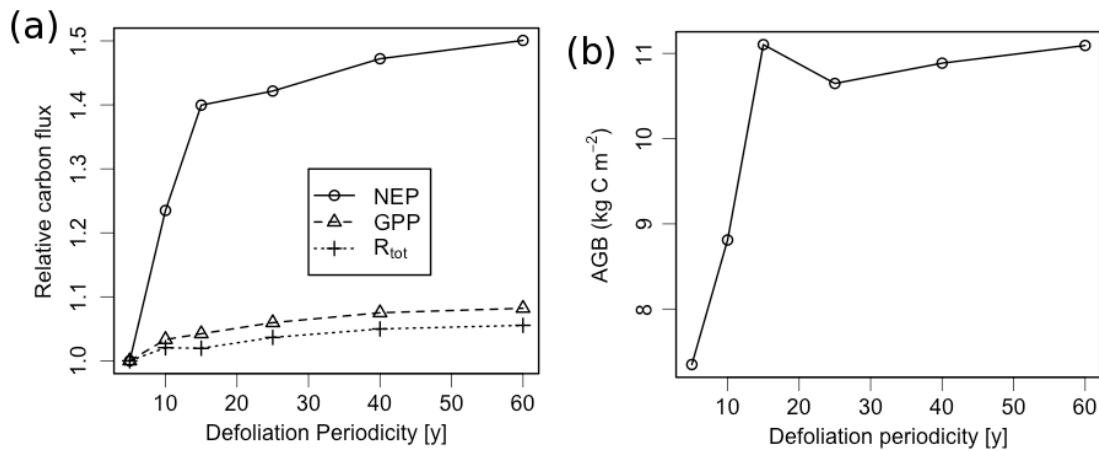


Figure 3. Impacts of defoliation periodicity on ecosystem carbon budgets. (a) Simulation-average impacts on gross primary productivity (GPP), total ecosystem respiration (R_{tot}), and net ecosystem productivity (NEP) are shown relative to the simulation average of I40-P5. (b) Live aboveground biomass (AGB) at the end of the 200 yr simulations.

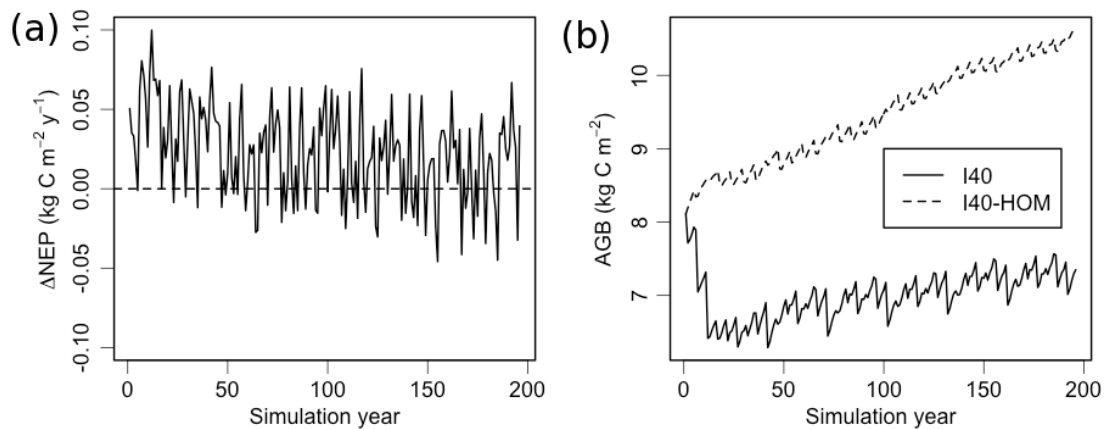


Figure 4. Ecosystem impacts due the spatial pattern of defoliation. (a) Annual net ecosystem productivity (NEP) from I40-P5-HOM minus the annual NEP from I40-P5. (b) Time series of live aboveground biomass (AGB) from the I40-P5-HOM and I40-P5.

However, I40-P5-HOM consistently has larger NEP than I40-P5, especially at the beginning of the simulation. Both runs have NEP values approaching zero toward the end of the simulations as the ecosystems approach their respective equilibria.

Throughout most of the simulated period, I40-P5-HOM has 20–30% more live AGB than I40-P5 (figure 4(b)). This arises because I40-P5-HOM has both greater GPP than I40-P5 (by 7% on the simulation average) and less mortality (by 44% on the simulation average). At the level of the entire canopy, the difference in GPP arises because of the nonlinear, saturating relationship between GPP and LAI. However, I40-P5 also has a distinct mortality peak every 5 yr following each defoliation event that is absent in I40-P5-HOM. In I40-P5-HOM, all oaks carry out some photosynthesis with >60% leaves throughout the defoliation event compensating for the lost foliage (VanderKlein and Reich 1999). After defoliation, the lost leaf biomass can in part be made up from the year’s photosynthate and from reallocation. In contrast, 40% of the oaks in I40-P5 cannot do any photosynthesis whatsoever during defoliation. After defoliation, these oaks have not accrued photosynthate to draw on, reallocation from

roots must fill a larger gap, and many oaks fall into negative carbon balance and may experience mortality. Moreover, the absence of carbon reserves may weaken oaks and allow for fungal attack. In the field, many oaks that died after the 2007 defoliation event at SLEF were observed to be ringed by basiocarpis in fall 2009.

4. Conclusions

This study investigates a spectrum of ways in which periodic gypsy moth outbreaks can affect forest biomass dynamics, functioning and composition on annual to century time scales. We address this issue by analyzing idealized simulations from a structured terrestrial biosphere model capable of representing the small-scale heterogeneity arising from disturbance, and we focus on SLEF as a case study because of its strong observational record. Few previous mechanistic models have successfully simulated changes in carbon cycling during these disturbances, and so one of our objectives here was to establish a baseline that can be evaluated in future studies.

We found that NEP decreased approximately linearly with increasing defoliation intensity, but live AGB and ecosystem composition exhibited strong nonlinearities. In the idealized scenario without defoliation, the ecosystem was more sensitive to drought and experienced more drought-induced mortality than in the more realistic scenarios that included defoliation. We also found a nonlinear response to disturbance periodicity for both NEP and live AGB, with ecosystem sensitivity generally being much larger for 5–15 yr periodicities than for 15–60 yr periodicities.

A major implication of this study is that it is essential to correctly specify the spatial and temporal patterns of defoliation events in order to accurately simulate the corresponding carbon dynamics. This is relevant to both historical and future outbreaks, and becomes particularly important when considering large spatial scales because regionally-averaged defoliation amounts can be much less than local defoliation amounts in patches. Partial defoliation of all stands was simulated to have a much weaker effect on site carbon budgets than a complete defoliation of some stands. In the case where each tree ‘pays’ for defoliation with the same fraction of its leaves, net carbon uptake is ~20% larger than the case where some trees ‘pay’ nothing and other trees are completely defoliated. This result highlights a challenge faced by aggregated terrestrial biosphere models that do not represent biotic heterogeneity resulting from disturbances, and thus overestimate NEP at larger spatial scales.

This study included idealized simulations to glean some insights into the century-scale impacts of frequency and intensity of gypsy moths defoliation on the carbon cycle. Actual ecosystem responses will depend on a range of complex factors including future drought frequency and severity, changes in the frequency of defoliation, and interactions with other disturbances, such as fire and windthrow. There is also uncertainty in the applicability of some of the details of our modeled defoliation events. For example, we prescribed the same temporal evolution of all defoliation events (figure 1). This was because we only had measurements at a sufficiently high temporal resolution for a single oak–pine forest defoliation event (SLEF in 2007). For simplicity in the model formulation, we also assumed that all oak trees in a defoliated stand share the same defoliation rate, while the pines are not defoliated at all. In future work, our model can be generalized to allow trees of size classes to be defoliated at different times, or to allow for the possibility of pine defoliation. Finally, our results were driven by information from one particularly well-measured site. In ongoing work, we are carrying out additional simulations to assess the regional-scale impacts of gypsy moth defoliation on the forests throughout the eastern US.

Acknowledgments

The authors are grateful for computational support provided by the PICSciE-OIT High Performance Computing Center and Visualization Laboratory at Princeton University. This

research was in part supported by USDA joint venture agreement 10-JV-11242306-136, NASA grant NNN08AH971, and the Office of Science (BER), US Department of Energy DE-SC0007041.

References

- Albani M, Medvigy D, Hurtt G C and Moorcroft P R 2006 The contributions of land-use change, CO₂ fertilization, and climate variability to the Eastern US carbon sink *Glob. Change Biol.* **12** 2370–90
- Albertson F W and Weaver J E 1945 Injury and death or recovery of trees in prairie climate *Ecol. Monogr.* **15** 393–433
- Amiro *et al* 2010 Ecosystem carbon dioxide fluxes after disturbance in forests of North America *J. Geophys. Res.* **115** G00K02
- Baker W L 1941 Effect of gypsy moth defoliation on certain forest trees *J. For.* **39** 1017–22
- Barron E S and Patterson W A III 2008 Monitoring the effects of gypsy moth defoliation on forest stand dynamics on Cape Cod, Massachusetts: sampling intervals and appropriate interpretations *For. Ecol. Manag.* **256** 2092–100
- Beaulieu C, Sarmiento J L, Mikaloff Fletcher S E, Chen J and Medvigy D 2012 Identification and characterization of abrupt changes in the land uptake of carbon *Glob. Biogeochem. Cycles* **26** GB1007
- Bréda N and Badeau V 2008 Forest tree responses to extreme drought and some biotic events: towards a selection according to hazard tolerance? *C. R. Geosci.* **340** 651–62
- Campbell R W and Sloan R J 1977 Forest stand responses to defoliation by the gypsy moth *For. Sci. Monogr.* **19** 1–34
- Clark K L, Skowronski N, Gallagher M, Renninger H and Schäfer K 2012 Effects of invasive insects and fire on forest energy exchange and evapotranspiration in the New Jersey pinelands *Agric. For. Meteorol.* **166/167** 50–61
- Clark K L, Skowronski N and Hom J 2010 Invasive insects impact forest carbon dynamics *Glob. Change Biol.* **16** 88–101
- Davidson C B, Johnson J E, Gottschalk K W and Amateis R L 2001 Prediction of stand susceptibility and gypsy moth defoliation in coastal plain mixed pine-hardwoods *Can. J. For. Res.* **31** 1914–21
- de Beurs K M and Townsend P A 2008 Estimating the effect of gypsy moth defoliation using MODIS *Remote Sens. Environ.* **112** 3983–90
- Edburg S L, Hicke J A, Lawrence D M and Thornton P E 2011 Simulating coupled carbon and nitrogen dynamics following mountain pine beetle outbreaks in the western United States *J. Geophys. Res.* **116** G04033
- Hicke J A *et al* 2012 Effects of biotic disturbances on forest carbon cycling in the United States and Canada *Glob. Change Biol.* **18** 7–34
- Hurtt G C, Pacala S W, Moorcroft P R, Caspersen J, Shevliakova E, Houghton R A and Moore B III 2002 Projecting the future of the US carbon sink *Proc. Natl Acad. Sci. USA* **99** 1389–94
- Johnson D M, Liebhold A M and Bjørnstad O N 2006 Geographical variation in the periodicity of gypsy moth outbreaks *Ecography* **29** 367–74
- Johnson D M, Liebhold A M, Bjørnstad O N and McManus M L 2005 Circumpolar variation in periodicity and synchrony among gypsy moth populations *J. Anim. Ecol.* **74** 882–92
- Kurz W A, Dymond C C, Stinson G, Rampley G J, Neilson E T, Carroll A L, Ebata T and Safranyik L 2008a Mountain pine beetle and forest carbon feedback to climate change *Nature* **452** 987–90

- Kurz W A, Stinson G, Rampley G J, Dymond C C and Neilson E T 2008b Risk of natural disturbances makes future contribution of Canada's forests to the global carbon cycle highly uncertain *Proc. Natl Acad. Sci. USA* **105** 1551–5
- Le Quéré C *et al* 2009 Trends in the sources and sinks of carbon dioxide *Nature Geosci.* **2** 831–6
- Liebhold A M, Halverson J A and Elmes G A 1992 Gypsy moth invasion in North America: a quantitative analysis *J. Biogeogr.* **19** 513–20
- Medvigy D and Moorcroft P R 2012 Predicting ecosystem dynamics at regional scales: an evaluation of a terrestrial biosphere model for the forests of northeastern North America *Phil. Trans. R. Soc. B* **367** 222–35
- Medvigy D, Wofsy S C, Munger J W, Hollinger D Y and Moorcroft P R 2009 Mechanistic scaling of ecosystem function and dynamics in space and time: ecosystem demography model version 2 *J. Geophys. Res.* **114** G01002
- Medvigy D, Wofsy S C, Munger J W and Moorcroft P R 2010 Responses of terrestrial ecosystems and carbon budgets to current and future environmental variability *Proc. Natl Acad. Sci. USA* **107** 8275–80
- Miao Z, Lathrop R G Jr, Xu M, La Puma I P, Clark K L, Hom J, Skowronski N and Van Tuyl S 2011 Simulation and sensitivity analysis of carbon storage and fluxes in the New Jersey Pinelands *Ecol. Modelling Softw.* **26** 1112–22
- Moorcroft P R, Hurtt G C and Pacala S W 2001 A method for scaling vegetation dynamics: the ecosystem demography model (ED) *Ecol. Monogr.* **71** 557–85
- Pan Y *et al* 2011 A large and persistent carbon sink in the world's forests *Science* **333** 988–93
- Peltonen M, Liebhold A M, Bjørnstad O N and Williams D W 2002 Spatial synchrony in forest insect outbreaks: roles of regional stochasticity and dispersal *Ecology* **83** 3120–9
- Pfeifer E M, Hicke J A and Meddens A J H 2011 Observations and modeling of aboveground tree carbon stocks and fluxes following a bark beetle outbreak in the western United States *Glob. Change Biol.* **17** 339–50
- Schäfer K V R 2011 Canopy stomatal conductance following drought, disturbance and death in an upland oak/pine forest of the New Jersey Pine Barrens, USA *Front. Plant Sci.* **2** 1–7
- Schäfer K V R, Clark K L, Skowronski N and Hamerlynck E P 2010 Impact of insect defoliation on forest carbon balance as assessed with a canopy assimilation model *Glob. Change Biol.* **16** 546–60
- Scheller R M, Van Tuyl S, Clark K L, Hom J and La Puma I 2011 Carbon sequestration in the New Jersey Pine Barrens under different scenarios of fire management *Ecosystems* **14** 987–1004
- Skowronski N, Clark K, Nelson R, Hom J and Patterson M 2007 Remotely sensed measurements of forest structure and fuel loads in the Pinelands of New Jersey *Remote Sens. Environ.* **108** 123–9
- VanderKlein D W and Reich P B 1999 The effect of defoliation intensity and history on photosynthesis, growth and carbon reserves of two conifers with contrasting leaf lifespans and growth habits *New Phytol.* **144** 121–32
- Whittaker R H and Woodwell G M 1968 Dimension and production relations of trees and shrubs in the Brookhaven Forest, New York *J. Ecol.* **56** 1–25